Trajectory planning of parallel pouring mechanism for pouring robot

Long Li [1,2], Chengjun Wang [2*], Hongtao Wu [1]

[1]College of Mechanical and Electrical Engineering, Nanjing University of Aeronautics and Astronautics, Nanjing, 210016,China.

[2]Collge of Mechanical Engineering, Anhui University of Science and Technology, Huainan, 232001, China

270956876@163.com (L. Li)

67155946@qq.com (C. Wang)

mehtwu@126.com (H. Wu)

*Corresponding author. Chengjun Wang

Tel: 0086-1521-249-3900

E-mail address: 270956876@163.com

Address: College of Mechanical and Electrical Engineering, Nanjing University of Aeronautics and Astronautics, Nanjing, 210016, China.

Abstract: Aiming at the problem of singular area in the working space when designing the parallel casting mechanism of the pouring robot, and the sensitivity of the pouring liquid to the acceleration of the ladle, this paper proposes the genetic fusion algorithm of particle swarm optimization (GA-IPSO) with angle and distance observer to find the optimal control point. The numerical analysis shows that it is feasible to change the tilting angle of the ladle to make the ladle traverse the singular regions safely. According to the simplified method of single pendulum, the sloshing model of pouring liquid is established, and the segmented acceleration planning method considering the sloshing of the pouring liquid is proposed in combination with the characteristics of high-speed cam motion. Numerical and experimental studies show that the segmented acceleration planning method can make the parallel pouring mechanism reach the set position in the shortest time while moving along the planned trajectory, and ensure that the sloshing range of the pouring liquid is within the safe range.

Keywords: parallel mechanism, pouring robot, singularity, GA-IPSO, Sloshing of pouring liquid.

INTRODUCE

Pouring is the process of pouring the molten metal with high temperature from the ladle into the mould cavity. There are dust, vibration, noise and other harsh operating environment because of its direct operation to molten metal molten liquid, which threats to the safety of the personal security of workers, thus, various accidents are also common. In order to solve such problems, related scholars have carried out a lot of researches on the pouring robot, various types of automatic pouring equipments have been developed for the pouring process[1,2]. The parallel pouring mechanism of the designed new hybrid truss type pouring robot is studied in this paper[3], mainly for trajectory planning and acceleration planning.

At present, the research of robot trajectory optimization is mostly concentrated on the series robot[4,5,6], there are few research on the trajectory planning of parallel mechanism, and most of them focus on several typical parallel platforms, such as DELTA, Stewart. SHEN et al. have designed an algorithm to select excellent path points and constructed continuous trajectory paths[7]. Abdellatif et al. put forward an adaptive algorithm to get the shortest path of 6-DOF manipulator. Experimental results show that the algorithm can give the required speed and the corresponding driving force effectively[8]. Pugazhenthi et al. proposes an algorithm for the Stewart

platform which can maximize the structure stiffness and guarantee the workspace and singular constraints of the mechanism[9]. Sen et al. uses the variational method to give the parallel mechanism no singular path and to ensure that the actuator is within the specified length range[10]. Afroum et al. parameterizes the motion coordinates in the workspace of a 3 DOF DETLTA parallel robot, and uses a continuous two programming method to optimize the trajectory of the target position[11].

As early as 1996, Terashima et al.[12] studied the sloshing of ladle. The distribution parameter method of fluid was applied to the SOLA-MAC numerical simulation to describe the pouring process of the liquid. The result was used to guide the structure design of ladle to better suppress the sloshing of the pouring liquid; Then a simplified pendulum model[13] was proposed to make the design of the pouring sloshing control system easier. M. Hamaguchi[14] et al. studied the sloshing suppression of curve motion. H. Yamagata and S. Kaneko et al.[15] gave an optimized driving model to enable the residual sloshing of the fluid to be better suppressed after rapid movement. Ken'Ichi Yano et al.[16] use H^{∞} model to suppress the residual vibration of the ladle, and add a rotating controller to the active suppression of the sloshing of the liquid in the motion, and a good effect has been obtained.

The research mentioned above only aims at the research on the non singularity, stiffness, driving force and working time of several typical parallel mechanisms, and the translation motion is considered more, while few studies have been made on the coupling motion of rotation and translation. For the parallel pouring mechanism designed in this paper, due to the structural and singular characteristics of the parallel pouring mechanism, there is a coupling relationship between rotation and translation. Previous studies have shown less research on global acceleration time-varying sloshing suppression, and active suppression will increase the complexity of pouring systems. Therefore, this paper proposes a fusion path optimization algorithm, which gives the shortest path of any two points in the working space of the parallel pouring mechanism, and sets the angle observer and the safe distance observer to cross the singular regions by changing the pouring angle. After that, the distribution scheme of acceleration and angular acceleration is given based on the sloshing model of pouring liquid and the motion model of high speed cam, and the shortest operation time in the safe acceleration range is obtained.

1 STRUCTURE OF MOBILE HEAVY LOAD POURING ROBOT

1.1 The structure of the casting robot

(Location of Fig.1)

As shown in Fig.1, a hybrid truss type mobile heavy load pouring robot is proposed[3,17]. Because the ladle rotates around a certain axis during the pouring process. and in order to adapt to the complex pouring environment, it is hoped that the ladle will not shake in other directions. Therefore, the parallel unit is designed to be a 4-DOF parallel mechanism with 1-axis rotation and 3-axis translation. Based on the analysis of 3-UPU parallel mechanism (3-DOF), a new type of 4-UPU parallel mechanism is proposed to meet the requirements of the pouring operation.

1.2 Description of parallel pouring mechanism

As shown in Fig.2, the parallel manipulator of the heavy load pouring robot can be simplified as 4-UPU (U on behalf of a universal joint, P on behalf of a shifting pair) parallel mechanism. The upper platform is a fixed platform, installed in the heavy pouring robot beam, and the lower platform is a motion platform, which is connected with the ladle. The 4 branches are UPU structural kinematic chains. At the time of initial assembly， the plane *ABab* formed by the chain 1 and 2 and the upper and lower platforms is vertical to the fixed platform *ABCD*, and the angle between the moving platform *abcd* and the plane *ABab* is γ. The plane *CDdc* formed by the chain 3 and 4 and the upper and lower platforms, the angle between the fixed platform *ABCD* and the plane *CDdc* is Ψ, the angle between the moving platform *ABCD* and the plane *CDdc* is ψ. The fixed coordinate system ***O-XYZ*** located at the midpoint AB edge, ***Z*** axis is perpendicular to the fixed platform, ***Y*** axis coincides with *AB* edge, Point ***C*** is on the extension of the ***X*** axis, the moving coordinate system ***o-xyz*** is located at the midpoint *ab* edge, ***z*** axis is perpendicular to the moving platform, ***y*** axis coincides with *ab* edge, Point ***c*** is on the extension of the ***x*** axis, the ***y*** axis is parallel to the ***Y*** axis. *ob* length is *m*, *oc* length is *f*, *dc* length is *g*, *OB* length is *M*, *OC* length is *N*, *DC* length is *K*. *Aa*, *Bb*, *Cc* and *Dd* are d_1, d_2, d_3 and d_4 respectively.

(Location of Fig.2)

The U pair consists of R pairs (R stands for the rotating pair) whose two axes are perpendicular to each other, and the kinematic chain UPU is equivalent to the combination of the RRPRR joints. The axes of each chain kinematic pair are successively represented as $\boldsymbol{S}_{i1}$, $\boldsymbol{S}_{i2}$, $\boldsymbol{S}_{i3}$, $\boldsymbol{S}_{i4}$, $\boldsymbol{S}_{i5}$,(i=1, 2, 3, 4, for the simple diagram, only the axis of the chain 1 is marked). $\boldsymbol{S}_{i1}$ is consistent with the direction

of $\boldsymbol{y}$ axis, $\boldsymbol{S}_{i5}$ consistent with the direction of the $\boldsymbol{Y}$ axis, the angle between $\boldsymbol{S}_{i3}$ and $\boldsymbol{S}_{i4}$ is Θ_i, $\boldsymbol{S}_{i1} \perp \boldsymbol{S}_{i2}$, $\boldsymbol{S}_{i4} \perp \boldsymbol{S}_{i5}$, $\boldsymbol{S}_{12} /\!/ \boldsymbol{S}_{22}$, $\boldsymbol{S}_{32} /\!/ \boldsymbol{S}_{42}$。

2 SINGULARITY ANALYSIS OF A NEW 4-UPU PARALLEL POURING MECHANISM

The new 4-UPU parallel pouring mechanism is composed of multiple closed chains, and the geometric constraint equation can be expressed by vector loop relation.

$$\boldsymbol{Oo} + {}^{O}_{o}\boldsymbol{R}\boldsymbol{S}_{i5} = \boldsymbol{S}_{i1} + {}^{O}_{i}\boldsymbol{R}\boldsymbol{S}_{i3} \tag{1}$$

$$\dot{S}_{i3} = \left({}^{O}_{i}\boldsymbol{R}\boldsymbol{s}_{i3}\right)^{T} \dot{\boldsymbol{Oo}} + \left({}^{O}_{i}\boldsymbol{R}\boldsymbol{s}_{i3}\right)^{T} {}^{O}_{o}\boldsymbol{R}\tilde{\boldsymbol{\omega}}_{o}\boldsymbol{S}_{i5}, \tag{2}$$

$$\boldsymbol{\omega}_{i} = \frac{1}{S_{i3}}\tilde{\boldsymbol{s}}_{i3}\,{}^{O}_{i}\boldsymbol{R}^{T}\left(\dot{\boldsymbol{Oo}} + {}^{O}_{o}\boldsymbol{R}\tilde{\boldsymbol{\omega}}_{o}\boldsymbol{S}_{i5}\right), \tag{3}$$

In equation (1), the subscript ${}^{O}_{o}\boldsymbol{R}$ and ${}^{O}_{i}\boldsymbol{R}$ (i=1,..., 4) of the rotation matrix represents the transformation from the local coordinate system o or i to the O of the inertial coordinate system, $\boldsymbol{Oo}$= $(ox, oy, oz)^{\mathrm{T}}$. $\boldsymbol{s}_{i3}$ is the unit vector of the axis along the i3 moving pair, and S_{i3} represents the change of the rod length of the i3 moving pair. $\boldsymbol{\omega}_o$=(0, Ψ, 0), ω_i represents the angular velocity of the branch i. $\boldsymbol{s}_{45}$ represents the unit vector of the direction of the rotation drive axis. The Jacobian matrix of the new 4-UPU parallel pouring mechanism is:

$$\begin{bmatrix} \dot{S}_{13} \\ \dot{S}_{23} \\ \dot{S}_{33} \\ \omega_4 \end{bmatrix} = \boldsymbol{Jacob}\begin{bmatrix} \dot{\boldsymbol{Oo}} \\ \boldsymbol{\omega}_o \end{bmatrix}, \tag{4}$$

Where

$$\boldsymbol{Jacob} = \begin{bmatrix} \left({}^{O}_{1}\boldsymbol{R}\boldsymbol{s}_{13}\right)^{T} & \left({}^{O}_{1}\boldsymbol{R}\boldsymbol{s}_{13}\right)^{T} {}^{O}_{1}\boldsymbol{R}\tilde{\boldsymbol{S}}^{T}_{15} \\ \left({}^{O}_{2}\boldsymbol{R}\boldsymbol{s}_{23}\right)^{T} & \left({}^{O}_{2}\boldsymbol{R}\boldsymbol{s}_{23}\right)^{T} {}^{O}_{2}\boldsymbol{R}\tilde{\boldsymbol{S}}^{T}_{25} \\ \left({}^{O}_{3}\boldsymbol{R}\boldsymbol{s}_{33}\right)^{T} & \left({}^{O}_{3}\boldsymbol{R}\boldsymbol{s}_{33}\right)^{T} {}^{O}_{3}\boldsymbol{R}\tilde{\boldsymbol{S}}^{T}_{35} \\ \frac{1}{S_{43}}\boldsymbol{s}^{T}_{45}\tilde{\boldsymbol{s}}_{43}\,{}^{O}_{43}\boldsymbol{R}^{T}_{4} & \frac{1}{S_{43}}\boldsymbol{s}^{T}_{45}\tilde{\boldsymbol{s}}_{43}\,{}^{O}_{45}\boldsymbol{R}^{T}_{4}\,{}^{O}_{4}\boldsymbol{R}\tilde{\boldsymbol{S}}^{T}_{45} \end{bmatrix}. \tag{5}$$

$\boldsymbol{s}_{45}$ represents the unit vector of the axis of rotation.

The singularity of the mechanism can be analyzed by taking the determinant of Jacobian matrix as 0.

$$\det[\boldsymbol{Jacob}] = 0 \tag{6}$$

The parameters of the parallel pouring mechanism in the 1.2 section are brought to equation (5) and (6), $\boldsymbol{s}_{i3}$= $(0, 0, -1)^{T}$, $\boldsymbol{s}_{45}$= (0,

1, 0)^T. The Jacobi singular equation of the mechanism is obtained.

$$\begin{aligned}
&\frac{2n\csc\Psi\sec\Psi\left(m-M\right)EFG}{d_1d_2d_3H}=0,\\
&E=n\sin\gamma+oz,\\
&F=N+ox-n\cos\gamma,\\
&G=ox\sin\gamma+oz\cos\gamma,\\
&H=n^2-2n\cos\gamma\left(N+ox\right)+2n\bullet oz\sin\gamma\\
&\quad+\left(N+ox\right)^2+oz^2.
\end{aligned}\tag{7}$$

The singularity condition of the new 4-UPU parallel pouring mechanism can be obtained by equation (7). The conclusion is as follows:

1) m=M and Ψ=0°/90°, namely the fixed platform and the moving platform are rectangular in the plane *ABba* direction and the *CDdc* of the parallel mechanism coincides or is perpendicular to the fixed platform, the determinant value of ***Jacob*** is 0. This kind of singularity is called structural singularity, and the new 4-UPU mechanism should be designed to avoid it.

2) when E, F, G, H appear at any 0, the determinant value of ***Jacob*** may be 0. Further analysis shows that when the structure size is determined in equation (7), the variables are ox, oz and γ, indicating that the new 4-UPU parallel pouring mechanism is the singular of the position and attitude coupling of the XZ plane in the workspace, and the H=0 is rewritten as the equation about the γ_H.

$$\begin{aligned}
&\gamma_H=-\arctan\left(\frac{oz\left(N+ox\right)\left(n^2+\left(N+ox\right)^2+oz^2\right)-I}{n^3oz^2+(N+ox)I+n\cdot oz^2\left(\left(N+ox\right)^2+oz^2\right)}\right),\\
&I=\sqrt{-n^2oz^2(-n^2+\left(N+ox\right)^2+oz^2)}.
\end{aligned}\tag{8}$$

Where, The I in γ_H has no solution in the real number domain, so H is always not 0, and just look at the situation of E、F、G=0. Given workspace and mechanism size: -150 mm≤ox≤-50，-50 mm≤oy≤-50，-825 mm≤oz≤-425，-28°≤γ≤62°；M=374 mm，N=680 mm，m=330 mm，f=365 mm. Traversing the given workspace, we get the singular regions of E、F、H=0, as shown in Fig.3 and Fig.4.

(Location of Fig.3)

(Location of Fig.4)

As we can see in Fig.3 and Fig.4:

1) the singular regions appears in the XZ plane, no correlation with the Y direction. Therefore, the trajectory planning is only discussed in the XZ plane, and the Y direction method is the same.

2) A part of the singular regions (the inner area of the quadrangle in Fig. 4) runs through the whole workspace, the singular point distribution is a plane of deflection, which shows that the singular angle γ is continuously changed in the XZ plane, therefore, the method of changing the γ can be considered to make the ladle pass through the singular regions in a manner approaching the singular face. The other parts of the singular regions account for only about 10% of the workpace, and in actual work, the boundary usually does not arrive, so the trajectory planning is not considered.

3 OPTIMAL TRAJECTORY PLANNING BASED ON A HYBRID STRATEGY

3.1 Particle swarm optimization algorithm (PSO)

In the n-dimensional search space, there are p particles in the search space, and the location of i particle in the search space is expressed by vector $x_i=[x_{i1},..,x_{in}]^T$. $G=G(x_i)$ is the cost function of the specific problem, that is to evaluate the degree of fitness (optimization) of the particle i in the search space. Each particle will get an optimal solution through search space, that is, $pb_i=[pb_{i1},..., pb_{in}]^T$. PSO updates the global best location solution after each iteration, $gb=[gb_i,...,gb_n]^T$. In the k iteration, the individual and global optimal location update process is

$$\boldsymbol{pb}_i^k=\begin{cases}\boldsymbol{pb}_i^k & \text{if } G\left(\boldsymbol{pb}_i^{k-1}\right)\le G\left(\boldsymbol{pb}_i^k\right)\\ \boldsymbol{x}_i^k & \text{if } G\left(\boldsymbol{pb}_i^{k-1}\right)> G\left(\boldsymbol{pb}_i^k\right)\end{cases} \tag{9}$$

$$\boldsymbol{gb}^i\in\left\{\left(\boldsymbol{pb}_1^k,...,\boldsymbol{pb}_p^k,\boldsymbol{gb}^i\right)\middle|G\left(\boldsymbol{gb}^i\right)=\min\left(G\left(\boldsymbol{pb}_1^k\right),...,G\left(\boldsymbol{pb}_1^k\right),G\left(\boldsymbol{gb}^{i-1}\right)\right)\right\} \tag{10}$$

In the iteration process, the i particle moves at the speed $v_i=[v_1,...,v_{in}]^T$ in the search space. The velocity and position of each particle are corrected according to the equation 11,12:

$$v_{ij}^{k+1}=wv_{ij}^k+c_1rand_2()\left(pb_{ij}^k-x_{ij}^k\right)+c_2rand_2()\left(gb_j^k-x_{ij}^k\right), \tag{11}$$

$$x_{ij}^{j+1}=x_{ij}^{i+1}+v_{ij}^{k+1}. \tag{12}$$

In equation 11, 12, j=1,...,n. c_1 and c_2 are normal numbers, which are called acceleration factors. $rand_1$ and $rand_2$ are normal distribution functions between [0,1]; w is known as the inertia factor and usually take 0.1~0.9. And the larger the value, the stronger the global search ability. Conversely, the stronger the local search ability.

In order to avoid the prematurity of the PSO algorithm, this paper proposes an improved particle swarm optimization algorithm based on the point to point of trajectory planning, and an adaptive strategy is used to modify the particle moving velocity by using the orientation vector of trajectory planning starting point and end point. That is:

$$v_{ij}^{k+1} = wv_{ij}^{k} + c_1 rand_2()\Delta v_{ij}^{k1} + c_2 rand_2()\Delta v_{ij}^{k1}, \tag{13}$$

$$\begin{cases} \Delta v_{ij}^{k1} = \Delta_{ij}^{k1}\left(pb_{ij}^{k} - x_{ij}^{k}\right) \\ \Delta v_{ij}^{k2} = \Delta_{ij}^{k2}\left(gb_{j}^{k} - x_{ij}^{k}\right) \end{cases} \tag{14}$$

Revised Δv_{ij}^{k1} and Δv_{ij}^{k2} according to equation 15 and 16

$$\Delta v_{ij}^{k1} = \begin{cases} \zeta^{+}\Delta_{ij}^{(k-1)1}, \text{if } \cos\left\langle x_{ideal} - pb_{ij}^{k-1}, x_{ideal} - x_{ij}^{k-1}\right\rangle \\ \qquad \bullet\cos\left\langle x_{ideal} - pb_{ij}^{k}, x_{ideal} - x_{ij}^{k}\right\rangle > 0 \\ \zeta^{-}\Delta_{ij}^{(k-1)1}, \text{if } \cos\left\langle x_{ideal} - pb_{ij}^{k-1}, x_{ideal} - x_{ij}^{k-1}\right\rangle \\ \qquad \bullet\cos\left\langle x_{ideal} - pb_{ij}^{k}, x_{ideal} - x_{ij}^{k}\right\rangle < 0 \\ \Delta_{ij}^{(k-1)1}, \text{others} \end{cases} \tag{15}$$

$$\Delta v_{ij}^{k1} = \begin{cases} \zeta^{+}\Delta_{ij}^{(k-1)2}, \text{if } \cos\left\langle x_{ideal} - gb_{j}^{k-1}, x_{ideal} - x_{ij}^{k-1}\right\rangle \\ \qquad \bullet\cos\left\langle x_{ideal} - gb_{j}^{k}, x_{ideal} - x_{ij}^{k}\right\rangle > 0 \\ \zeta^{-}\Delta_{ij}^{(k-1)2}, \text{if } \cos\left\langle x_{ideal} - gb_{j}^{k-1}, x_{ideal} - x_{ij}^{k-1}\right\rangle \\ \qquad \bullet\cos\left\langle x_{ideal} - gb_{j}^{k}, x_{ideal} - x_{ij}^{k}\right\rangle < 0 \\ \Delta_{ij}^{(k-1)2}, \text{others} \end{cases} \tag{16}$$

In the equation 15 and 16, x_{ideal} represents the ideal location vector of the starting point to the end point. cos< , > represent the cosine of the direction vector.

The ideal position vector from the starting point to the end point is used as the target direction vector, in equation 15 and 16, when the cosine direction of the two difference calculation of the particle is the same, it shows that the particle is approaching to one side of the individual (global) extremum. At this time, it can increase $\Delta_{ij}^{(k-1)1}$ ($\Delta_{ij}^{(k-1)2}$) to speed up the convergence rate of the algorithm and take the increasing factorζ^{+}; If the cosine direction of the two difference calculation is inconsistent, it is shown that the particle is hovering near the individual (global) extremum, then ζ^{+} can be reduced to avoid particles linger around the extremum and lead to premature algorithm; If the cosine directions of the two difference calculation of the particles coincide, then $\Delta_{ij}^{(k-1)1}$ ($\Delta_{ij}^{(k-1)2}$) is not changed, $0<\zeta^{-}<1<\zeta^{+}$.

3.2 Angle observer

Through the analysis of *E*, *F* and *H*, the singularity of 4-UPU is related to *ox*, *oz*, γ. In order to cross the singular regions, the planning strategy of changing γ is adopted, that is, by changing the tilting angle of the ladle, the $E \bullet F \bullet G \neq 0$ will be ensured to ensure that the parallel pouring mechanism passes through the singular region smoothly. The specific search process is as follows:

Initialization:$\gamma = \gamma_0$

for *j*=1,2...,*n*

(1) $(ox, oz) \leftarrow x_{ij}^k$

(2) **if** $E \bullet F \bullet G=0$

(3) Initialization:$\gamma^+ = \gamma^- = \gamma$，$\gamma_0$

(3) **whlie** $E \bullet F \bullet G \neq 0$

(a)$\gamma^+ = \gamma^+ + \nabla_1$ &&$\gamma^+ < \gamma_0$

(b)$\gamma^- = \gamma^- - \nabla_1$

(c)$\gamma = (\gamma^-, \gamma^+)$, First to meet $E \bullet F \bullet G \neq 0$

end

end

γ_0 is the titling angle of the ladle during the initial movement. In the above singular regions search process, the dip angle searches for the minimum increase (reduction) of ∇_1 in two directions, but the increase can not exceed the initial tilt angle of γ_0, because in the actual operation, exceeding γ_0 will cause splashing of ladle and cause serious safety accidents.

3.3 Distance observer

Combined with the actual working environment analysis, the most common type of collision is the ladle and the pouring cup. The method used in this paper, as shown in Figure 5, the distance *r* between the center of the ladle and the edge of the pouring cup is the minimum safe distance. The specific search process is as follows:

(Location of Fig.5)

for *j*=1,2...,*n*

(1) $(ox,oz) \leftarrow x_{ij}^{k}$

(2)look for $pcx_{\min}$, $pcz_{\min}$

(2)**if** $\left(ox - pcx_{\min}\right)^2 - \left(oz - pcz_{\min}\right)^2 \geq r^2$

(3)**while** $\left(ox - pcx_{\min}\right)^2 - \left(oz - pcz_{\min}\right)^2 < r^2$

(a)$ox=ox+\nabla_2$

(b) $oz = pcz_{\min} - \dfrac{oz_0 - pcz_{\min}}{ox_0}\left(pcx_{\min} - ox\right)$

end

(4) $x_{ij}^{k} \leftarrow (ox,oz)$

end

$pcx_{\min}$, $pcz_{\min}$ is the nearest point of the tilting center of the ladle and the edge of the pouring cup. The positive and negative of the increment ∇_2 depends on the direction of movement of the ladle.

3.4 GA-IPSO algorithm

The flow chart of the GA-IPSO algorithm is shown in Fig. 6.

(Location of Fig.6)

Random dimensionality reduction: A large number of control points are necessary to fit the path, the efficiency of the algorithm will be reduced, so the dimension of individual position vectors is reduced randomly to improve the efficiency of the algorithm. The specific process is as follows:

$$\left[x_{i1}^{k}, x_{i2}^{k} \ldots, x_{in}^{k}\right]^{T} \xrightarrow[\left[x_{in_1}^{k}, \ldots, x_{in_2}^{k}\right]^{T}]{\text{Random}} \left[x_{i1}^{k}, \ldots, x_{i(n-(n_2-n_1+1))}^{k}\right]^{T} \tag{16}$$

In Equation 16, The n_1~n_2 positions are randomly deleted from the position vector of the individual, and the remaining n-(n_2-n_1+1) dimensional position vector recombination continues to solve the algorithm.

4 NUMERICAL ANALYSIS

a. Size and layout of parallel pouring mechanism and pouring cup

The parallel pouring mechanism adopts the design size, the workspace and the singular regions in section 2. The size of the gate cup is selected in the document [18]. In order to have both distance collision and singular path planning, and the layout is like Fig.7.

(Location of Fig.7)

b. cost function

The cost function is defined as:

$$\boldsymbol{G}=\delta\boldsymbol{\psi}(\ \boldsymbol{pb}_i^k\ )+(1-\delta)\boldsymbol{\varphi}(\ \boldsymbol{pb}_i^k\ ) \tag{17}$$

In equation 17, $\boldsymbol{\psi}(\ \boldsymbol{pb}_i^k\ )$ represents the k iteration path length (step number) of the particle i, and $\boldsymbol{\varphi}(\ \boldsymbol{pb}_i^k\ )$ represents the step number of the angle change in the k iteration path of the particle i. The algorithm takes the sum of the distance and the step of the angle as the cost function. The δ is a weight coefficient with a range of $0\leq\delta\leq1$. When δ =0 represents the minimum angle problem, δ=1 represents the minimum path problem.

c. algorithm assignment

In order to ensure the appropriate speed of maturation, w,r_1 and r_2 in equation 13 are 0.6,1.2,1.2 respectively, ζ^+ andζ^- are 0.8,0.2 respectively, and the initial Δ_{ij}^{11} and Δ_{ij}^{21} are 1. The variation rate p_m and the cross rate p_c were 0.2,0.5, respectively. The initial position x_{i1}^k and target position x_{in}^k of the moving platform are x_{i1}^k =[-140, -690], x_{in}^k =[-65 and -545] respectively, and the angle of initial tilting is γ =20° . The number of particles is p=40. The algorithm terminates conditions: (1) the maximum number of iterations is 1000 times, or (2) in the two successive iterations, the fitness of the best particles is less than 1. The incremental ∇_1 of the distance observer and the incremental ∇_2 of the angle observer are 1 mm and 0.1 °respectively, smaller ∇_2 values can ensure the correctness and continuity of angle fitting. Properly amplify the minimum security distance and take r=430 mm.

Due to the acceleration method in Section 3.4 and the quality requirements of the algorithm in the singular regions, the number of the initial control points (the dimension of the position vector) is 180, and the number of the minimum control points (the dimension of the position vector) is 60. The algorithm is compiled into Matlab, and the control points are all rounded. The result is fitted by a simple B spline curve.

(Location of Fig.8)

(Location of Fig.9)

(Location of Fig.10)

(Location of Table 1)

(Location of Table 2)

Table 1 shows the comparison of different δ in GA-IPSO algorithm in path planning. The simulation of Table 1 runs on a Xeon E5 2.10GHz computer and takes the average of 10 simulation results. The computing time is directly used by MATLAB's own "*cputime*" function. The range of the δ is δ=0~1, where the δ=0 is equivalent to the minimum rotation angle of the ladle, while the δ=1 is equivalent to the shortest path problem. Table 1 path planning results corresponding to different weighting factors such as Fig.8, Fig.9 and Fig.10, in which Fig.9 and Fig.10, we use *z* and *x* as base coordinates in order to express the rotation angle.

In Table 1, with the decrease of δ, the number of iterations, calculation time and fitness are significantly improved. Combined with Fig.8, Fig.9 and Fig.10 , it can be seen that this is due to the increase of the weight factor of the ladle angle, which leads to a large deviation of the trajectory of the ladle from the pouring cup, the process of the singular regions and the rotation angle of the ladle are shortened, the correction times of the distance observer and angle observer decrease, thus accelerating the convergence of iteration, but the δ =0 and δ=0.2 obviously are not the desired trajectories, because they deviate from the ideal trajectory (straight path); When δ=1, the number of iterations, calculation time and fitness value are the largest, and the algorithm efficiency is poor; When δ=0.8 and δ=0.5, the trajectory is close, and the calculation time and fitness value of the algorithm are also close and moderate. Therefore, δ=0.5~0.5 is selected as the best compromise for the two competitive targets in the GA-IPSO algorithm (trajectory and ladle rotation angle).

Table 2 is the comparison between the standard PSO algorithm and the GA-IPSO algorithm in δ=0.5, and the particle number *p*=40. It can be seen from table 2 that GA-IPSO is not only efficient in computation but also in the quality of the final value compared with the standard PSO.

5 ACCELERATION PLANNING CONSIDERING SLOSHING OF POURING LIQUID

5.1 Pendulum-type Model

In order to facilitate the combination of the sloshing model and the acceleration model of the trajectory, this paper intends to use the pendulum method to establish the sloshing model of the pouring liquid, as shown in Fig.11.

In Fig.11, o_f-x_f-z_f is a liquid surface coordinate system $\overline{o_f x_f}$ is parallel to the horizontal plane. o_r-x_r-z_r is located in the rotating fulcrum coordinate system, $\overline{o_r x_r}$ is parallel to the horizontal plane, m_f is the quality of pouring liquid, c_f is the equivalent damping, l_f is the equivalent pendulum length, η is the pouring angle, φ is the sloshing angle of pouring liquid, ϕ(ϕ=η+φ) is the sloshing angle relative to the horizontal plane, o_r is the center of rotation,, o_g is the center of mass of pouring liquid, D_f is the distance between o_r and o_g, o_f is the pivot of the pendulum, θ_g is the angle between $\overline{o_r o_g}$ and the horizontal, and θ_g is the angle of the acceleration a_f and the horizontal, J is the moment of inertia, J= $m_f l_f^2$. The pendulum sloshing equation of the pouring liquid at the o_f point can be written as

$$\begin{aligned} J\frac{\mathrm{d}^2(\eta+\varphi)}{\mathrm{d}t^2} = &-c_f\frac{\mathrm{d}\left\{l_f(\eta+\varphi)\right\}}{\mathrm{d}t}l_f\cos(\eta+\varphi) \\ &- m_f g l_f \sin(\eta+\varphi) \\ &- m_f\frac{\mathrm{d}\left\{\left(D_f\cos\theta_g\right)\eta\right\}}{\mathrm{d}t^2}l_f\sin(\eta+\varphi) \\ &- m_f\frac{\mathrm{d}\left\{\left(D_f\sin\theta_g\right)\eta\right\}}{\mathrm{d}t^2}l_f\cos(\eta+\varphi) \\ &\text{-}m_f a\cos(\theta_a)l_f\cos(\eta+\varphi) \\ &+ m_f a\sin(\theta_a)lf\sin(\eta+\varphi) \end{aligned} \tag{18}$$

(Location of Fig.11)

For ϕ=η+φ, due to the small amplitude of the sloshing of the pouring liquid, the linearization of equation 18 can be obtained directly.

$$\ddot{\phi} = -\frac{c_f}{m_f}\dot{\phi} - \frac{g}{l_f}\phi - \frac{D_f\sin\theta_g}{l_f}\ddot{\eta} - \frac{a_f\cos\theta_a}{l_f} \tag{19}$$

By the pendulum characteristic, we can get the natural frequency ω_n and the damping coefficient ζ:

$$\omega_n = \sqrt{\frac{g}{l_f}}\ ,\quad \zeta = \frac{c_f}{2m}\sqrt{\frac{l_f}{g}} \tag{20}$$

In equation (20), ω_n and ζ can be easily measured by experimental, and can be estimated by equation 21 and 22[20, 21], d_1 is the depth of liquid, υ is the viscosity of liquid, B_1 is the average width of ladle, and L_f is the distance between o_r and o_f.

$$\zeta = d_1 \upsilon^{1/2} (B_1 / 2)^{-3/4} g^{-1/4} \tag{21}$$

$$L_f / l_f \approx 2 \sim 3 \tag{22}$$

5.2 Acceleration planning

Referring to the motion law of high speed cam[19], the acceleration planning requirements under the condition of sloshing are proposed: (1) The speed and acceleration of the parallel pouring mechanism at starting, stopping and folding point are all 0. (2) The jerk is 0 when the ladle is stopped. (3) Since the partial translational motion is accompanied by the rotation of the ladle, in order to reduce the acceleration variation of the composite motion, the pure translational motion time: the ratio of the translational + rotational motion time is 3:7.

Write down the boundary conditions according to the requirements:

$$s_{t0}(0)=v_{t0}(0)=a_{t0}(0)=0 \tag{23}$$

$$s_{tn}(1)=1 \tag{24}$$

$$v_{tn}(0)=a_{tn}(0)=j_{tn}(0)=0 \tag{25}$$

$$t_{tT}:t_{tTR}=3:7 \tag{26}$$

$$\text{Additional constraints}\begin{cases} s_{t2}(t_2)=l_{t2},\ v_{t2}(t_2)=a_{t2}(t_2)=0 \\ s_{t3}(t_3)=l_{t3},\ v_{t3}(t_3)=a_{t2}(t_2)=0 \\ \cdots \end{cases} \tag{27}$$

s_{ti}, v_{ti}, a_{ti} and j_{ti} in 23~27 are path length, speed, acceleration and jerk (i=0,1,2,..., n) respectively. t_{tT} and t_{tTR} are translation time and compound motion time, and the displacement function is n-1 order polynomial.

$$s_t = \rho_0 + \rho_1 t + \rho_2 t^2 + \ldots + \rho_{n-1} t^{n-1} \tag{28}$$

In equation 28, ρ_0, ρ_1, ρ_2,..., ρ_{n-1} are coefficients of polynomials. According to equation 28, we can get v_t, a_t, j_t by continuous derivating.

5.2.1 Translation path acceleration planning

Translation is the main movement form of ladle, so it is the emphasis of acceleration planning. Assign the model in Figure 11 to the actual operating conditions, d_1=0.37m， $\upsilon = 1.0067 \times 10^{-6}$ m^2/s, The upper and lower diameters of the inner cavity of the ladle are 0.52 m, 0.47 m and the height is 0.54 m, B_1=0.486 m，ζ=6.06×10^{-4}. L_f/l_f takes an average of 2.5, L_f=0.1 m, and l_f=0.04 m. D_f=0.085 m, θ_g =-1.919 rad. At the initial time, $\phi(0)$=0， $\phi'(0)$=0. The preferred path and angle parameters are obtained when δ=0.5 is taken.

a) Global acceleration planning

The normal acceleration planning is to plan the whole path. When δ =0.5, the path length is 0.174 m. Because the arc line of the path is only 0.005 m, it has less influence on sloshing, for straight-line processing, then the length of each broken line is 0.103m, 0.014m, 0.016 m, and 0.044 m respectively. According to the acceleration plan proposed in 5.2, we can get :

$$s_{t0}(0)=v_{t0}(0)=a_{t0}(0)=0 \tag{29}$$

$$s_{t5}(1)=1 \tag{30}$$

$$v_{t5}(0)=a_{t5}(0)=j_{t5}(0)=0 \tag{31}$$

$$\text{Additional constraints}: \begin{cases} s_{t2}(0.569)=0.592,\ v_{t2}(0.569)=a_{t2}(0.569)=0 \\ s_{t3}(0.683)=0.655,\ v_{t3}(0.683)=a_{t2}(0.683)=0 \\ s_{t5}(0.849)=0.747,\ v_{t3}(0.849)=a_{t2}(0.849)=0 \end{cases} \tag{32}$$

The equation 29~32 is introduced into Matlab and the global acceleration is obtained. The acceleration change in unit time is shown in Fig.12. The global acceleration planning scheme has the following disadvantages:

1. The peak acceleration is extremely large, it will increase the burden of the drive unit of the parallel mechanism; The acceleration in the first half is acute change, and the second half is basically zero, and the entire period is not fully utilized.

2. the fitting polynomial of acceleration is as high as 13 times, increasing the operation time.

(Location of Fig.12)

$$T_{\text{total}}=\sqrt{\frac{A_{\max}\times s_{\text{total}}}{a_{\max}}} \tag{33}$$

In equation 33, $A_{\max}$ is the maximum acceleration in unit time. s_{total} is the total length of a given path, $a_{\max}$ is the maximum acceleration of a given path, and T_{total} is the total time required to traverse the path at a given $a_{\max}$.

b) Piecewise acceleration planning

In view of the sensitivity of the pouring liquid to impact vibration, a piecewise planning method with breaking points as the starting point and ending point is proposed.

$$\begin{cases} s_{te0}(0)=0,\ v_{te0}(0)=a_{te2}(0)=0 \\ a_{te2}(0.3)=0,\ s_{te3}(1)=1 \\ v_{te3}(1)=a_{te3}(1)=j_{te3}(1)=0 \end{cases} \tag{34}$$

In equation 34, e=1,2,3,4. In pouring ladle movement, it is hoped that the pouring liquid will have longer sloshing buffer time in each part, so as to adapt to the next acceleration change better, and make $a_{te2}(0.3)=0$. Bring the equation 34 into Matlab and get the

acceleration of each segment:

$$a_{te}=1235.294t^5-3829.412t^4+4249.412t^3-1951.765t^2+296.471t \quad (35)$$

$$A_{\max\_e}=14.112 \quad (36)$$

In equation 36, $A_{\max\_e}$ represents the maximum acceleration of unit time within each planning segment of the path. Fig.13 is the variation of acceleration in unit time during piecewise acceleration planning. It can be seen that in the actual acceleration fitting, the unit acceleration peak of the piecewise acceleration planning is very small, the burden of the drive unit of the parallel mechanism is less. The time required for each segment of acceleration to reach the peak is very short, thereafter, the change of the acceleration is slow, which makes full use of the whole time. The fitting polynomial of acceleration is only 8 times, and the speed of operation is fast.

(Location of Fig.13)

Therefore, in this paper, a piecewise acceleration planning strategy is applied to the acceleration planning of the translational path. The actual acceleration a_{te_A} of each segment is:

$$a_{te\_A}=\frac{a_{\max}}{A_{\max}}\begin{pmatrix}1235.294\tau^5-3829.412\tau^4+4249.412\tau^3\\-1951.765\tau^2+29\ 6.471\tau\end{pmatrix},$$

$$\tau=\frac{t}{T_{\text{total}}}. \quad (37)$$

5.2.2 Rotational acceleration planning

The acceleration of rotational is also divided by piecewise planning. In Fig.9 and Fig.10, the change of the tilting angle is one-to-one correspondence with the change of the translation path. Therefore, the corresponding relations between rotation and translation in Fig.9 and Fig.10 can be directly used for polynomial fitting.

5.3 Experimental verification

First, we use the acceleration planing in the 5.2 section to planing the acceleration of the path. At δ=0.5, the θ_a of ladle is 1.221 rad, 1.954 rad, 0.139 rad and 0.872 rad respectively. Further analysis of formula 19 shows that $D_f\sin\theta_g/l_f$=0.725 and $\cos\theta_a/l_{f\ (\min)}$=8.565, which indicates that rotational acceleration has little effect on sloshing. In addition, the prototype is still in the design and processing stage. Therefore, the validation experiment only makes acceleration planning for translation path.

The verification experiment was performed on a six-free series robot. Since the kinematic viscosity of water is similar to the

kinematic viscosity of molten cast iron and is readily available in the laboratory, water is selected as the research fluid. The experimental setup is shown in Fig.14. This experiment mainly studies the sloshing state of the liquid in the container under the translational state, so in formula 19, the sloshing angle of the liquid is measured by the measurement method shown in Fig.15. The sloshing angle according to formula 38.

$$\phi = \arctan \frac{(dp_2 - dp_1)}{\frac{Bp}{2}} \tag{38}$$

In the formula 38, dp_1 and dp2 are liquid level heights, and B_p is the distance between the liquid level sensors. The trajectory of a container moves along the preferred path at δ=0.5 in Section 4. The sloshing law of the liquid in the container and the acceleration change of the end of the robot are obtained by the pendulum model and the piecewise acceleration model in Section 5. The maximum acceleration at each stage is calculated to be 1.39 m/s^2, 1.07 m/s^2, 0.24 m/s^2, 0.36 m/s^2, and the maximum sloshing angle is 0.08 rad. Numerical simulation and experimental results are shown in Fig. 16.

(Location of Fig.14)

(Location of Fig.15)

(Location of Fig.16)

(Location of Fig.17)

Comparing the numerical simulation results and experimental results in Fig.19: 0 s~2.91 s is the sloshing state of the water in the container during the robot movement time, and 2.91 s~5 s is the free sloshing of the container at the target position. The sloshing amplitude obtained by the experiment in 0 s~5 s is slightly attenuated because the viscous resistance of the water and the wall of the container is not considered in the model. However, the form and frequency of sloshing are basically the same, and the sloshing angle does not exceed the maximum threshold. It indicates that the liquid sloshing and acceleration planning methods in Sections 4 and 5 have higher operating efficiency and can prevent splashing accidents caused by severe sloshing. Fig.17 shows the instantaneous sloshing state of the water in the container, corresponding to the instantaneous sloshing amplitude in Fig.16, and the instantaneous liquid level sloshing is stable without violent fluctuation.

6 CONCLUSION

In this paper, a new 4-UPU parallel pouring mechanism with 4 DOF for casting robot is studied, and a path planning method and acceleration planning method are proposed. The main work and conclusions are as follows:

(1) By studying the singularity of 4-UPU parallel pouring mechanism, propose the GA-IPS algorithm with angle observer, position observer, speed corrector and flexible control points. The numerical example shows the feasibility of crossing the singular region and the correctness of the algorithm.

(2) Based on the motion characteristics of the high-speed cam and the sloshing characteristics of the pouring liquid, the method of acceleration planning is studied. In the view of the obvious characteristics of the impact vibration of the pouring liquid, the feasibility of the piecewise acceleration planning method under the constraints of speed, acceleration and jerk is proposed and verified.

(3) Based on the single pendulum model, the damping pendulum model of the rotation and moving fusion of the pouring liquid under the small sloshing condition is established, and fitting with the piecewise acceleration model, the maximum value of acceleration in each stage is given by the search method. The method of fitting the rotational acceleration is given by means of the relationship between the path and the tilting angle. The experimental results also verify the correctness of the established single pendulum model and acceleration model.

ACKNOWLEDGE

Thanks for the support of the major science and technology projects in Anhui China: The development of heavy-load casting robot in complex operation environment (Grant No.16030901012) ; Thank you for the support of "Postgraduate Research & Practice Innovation Program of Jiangsu Province (Grant No. KYCX18_0260)".

REFERENCE:

1. Kozuszek, K., Robotic problem solving. *Modern Casting*, 2006, 96(4), 24-28.

2. Terashima, K., Recent automatic pouring and transfer system in foundries. *Sokeizai*, 1998, 39, 1-8.

3. Wang, C., Li, L., Guo, Y. and Sheng, Y., *Hybrid trussed mobile heavy duty casting robot*. China Patent, 201710-682226.8(2017).

4. Chettibi, T., Lehtihet, H. E., Haddad, M., Hanchi, S., Minimum cost trajectory planning for industrial robots. *European journal of mechanics*. 2004, 23(4), 703-715.

5. Constantinescu, D. and Croft, E. A., Smooth and time‐optimal trajectory planning for industrial manipulators along specified paths. *Journal of robotic systems*, 2000, 17(5), 233-249.

6. Park, J. and Bobrow, J. E., Reliable computation of minimum‐time motions for manipulators moving in obstacle fields using a successive search for minimum‐overload trajectories. Journal of Field Robotics, 2005, 22(1), 1-14.

7. Dasgupta, B., Singularity-free planning for the Stewart platform manipulator. *Mech. Mach. Theory*, 1998, 33, 771-725.

8. Abdellatif, H., and Heimann, B., Adapted time-optimal trajectory planning for parallel manipulators with full dynamic modeling. In Proceedings of the 2005 IEEE International Conference on, Barcelona, Spain, 2005.

9. Pugazhenthi, S., Nagarajan, T. and Singaperumal, M., Optimal trajectory planning for a hexapod machine tool during contour machining. *Proceedings of the Institution of Mechanical Engineers, Part C: Journal of Mechanical Engineering Science*, 2002, 216(12), 1247-1257.

10. Sen, S., Dasgupta, B. and Mallik, A. K,. Variational approach for singularity-free path-planning of parallel manipulators. *Mechanism and Machine Theory*, 2003, 38(11), 1165-1183.

11. Afroun, M., Chettibi, T. and Hanchi, S., Planning optimal motions for a DELTA parallel robot. In Proceedings of the 14th Mediterranean Conference on Control and Automation, Ancona, Italy, 2006.

12. Terashima, K., Kaneshige, A., Koyamatsu, H., Yamaura, K., Ronda, W. Y. and Inagaki, T., Modeling and Motion Control of Fluid Behavior in Automatic Pouring System. *IFAC Proceedings Volumes*, 1996, 29(1), 6197-6202.

13. Terashima, K., Hamaguchi, M. and Yamaura, K., Modeling and input shaping control of liquid vibration for an automatic pouring system. In Proceedings of 35th IEEE Conference on Decision and Control, Kobe, Japan,1996.

14. Hamaguchi, M., and Yamamoto, M. and Terashima, K., Modeling and control of sloshing with swirling in a cylindrical container during a curved path transfer. In Proceedings of the 2nd Asian Control Conference, Tokyo, Japan, 1997.

15. Yamagata, H. and Kaneko, S., Sloshing Suppression Control of Contained Liquid in a Moving Cylindrical Container. *Trans. JSME*., 1997, 64(621), 671-674.

16. Yano, K. I. and Terashima, K., Robust liquid container transfer control for complete sloshing suppression. *IEEE Transactions on Control Systems Technology*, 2001, 9(3), 483-493.

17. Li, L., Wang, C. and Wu, H., Research on Kinematics and Pouring Law of a Mobile Heavy Load Pouring Robot. *Mathematical Problems in Engineering*, 2018.

18. Pan, X. and Xu, Y. Figures Selecting the Basin in Investment Casting. *Special-cast and Non-ferrous Alloys*, 1996 (5), 34-36.

19. Zhang, C., High - speed CAM mechanism commonly used movement law. In *Mechanical dynamics*(ed. Zhang, C.), Higher Education Press, China, 2008, pp. 137-143.

20. Binjie, M. and Hong, L., Analysis of Harmonic Response of Liquid Sloshing. *Missiles and Space Vehicles*, 2005, 1, 008.

21. Chen, J., Zhu, H., Zhang, L. and Sun, Y., Research on fuzzy control of path tracking for underwater vehicle based on genetic algorithm optimization. *Ocean Engineering*, 2018, 156, 217-223.

Table Captions

Table 1 Performance analysis of planned trajectories for various weighting factors δ

Particle no.	40				
δ	1	0.8	0.5	0.2	0
No. of iterations	553	488	413	387	321
Computiontion time(sec)	1182	1022	926	774	664
Fitness value	178	149	132	110	80

Table 2 Comparison of Standard PSO algorithm and GA-IPSO for weighting factor δ=0.5

Optimization	Standard PSO	GA-IPSO
No. of iterations	791	413
Computiontion time(sec)	1673	926
Fitness value	141	132

Figure Captions

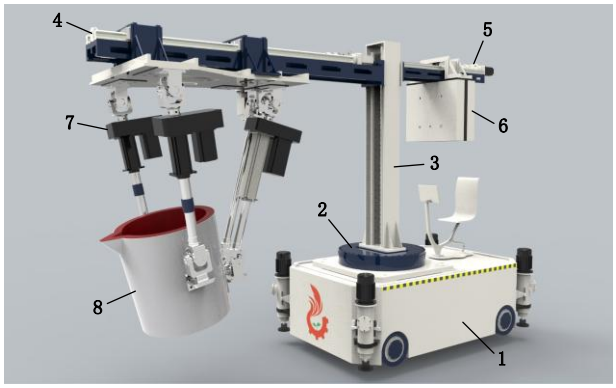

1. 4WD mobile platform 2. Slewing device 3. Hoisting device 4. Forward device 5. Backward device 6. Counterweight device 7. Parallel manipulator 8. End-effector

Fig.1. Hybrid truss type movable pouring robot

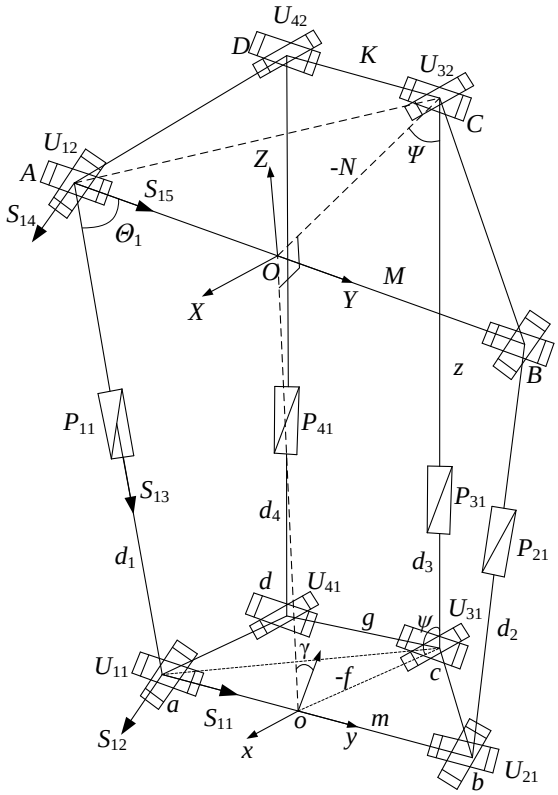

Fig.2. Schematic diagram of 4-UPU parallel manipulator for pouring robot

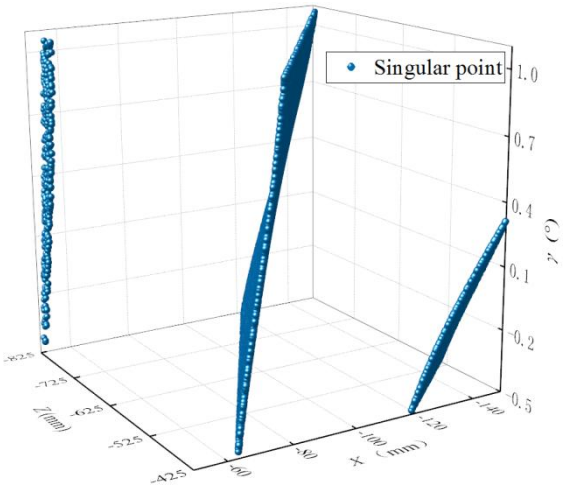

Fig.3. Singular regions of position and pose coupling in workspace

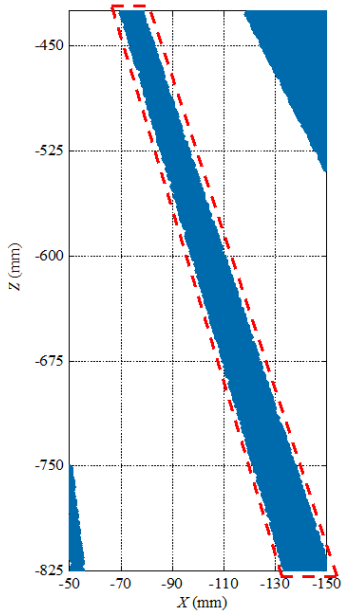

Fig.4. The projection of a singular regions in the direction of *XZ*

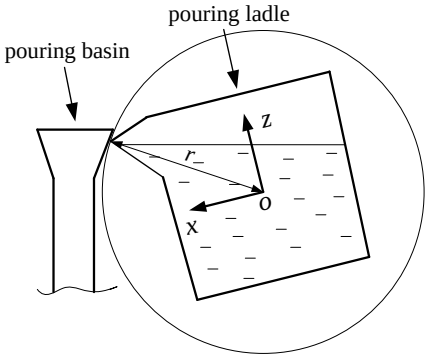

Fig.5. A schematic diagram of a collision between a ladle and a pouring cup

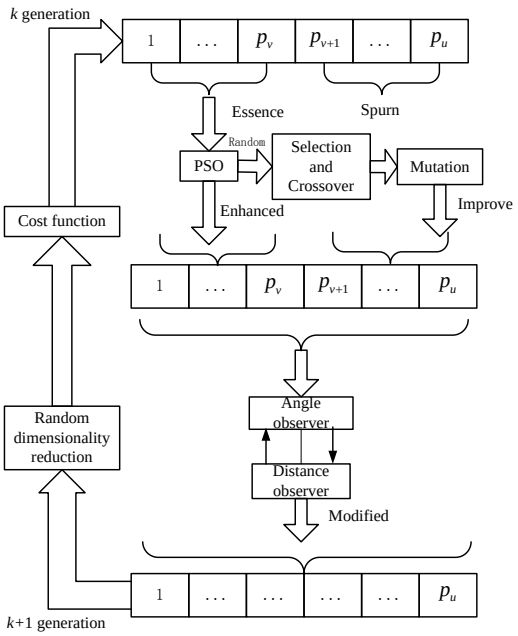

Fig.6. Flow chart of the GA-IPSO algorithm

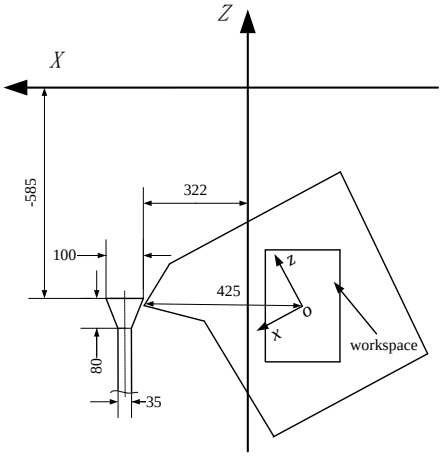

Fig.7. The size and layout of the pouring cup

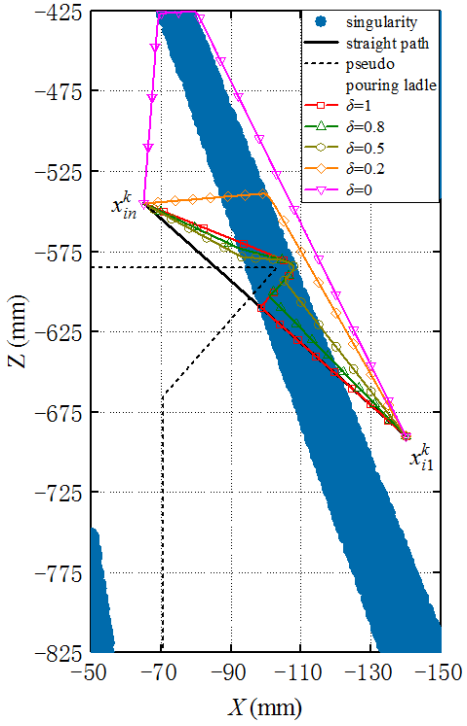

Fig.8. Planning path of different weight factors

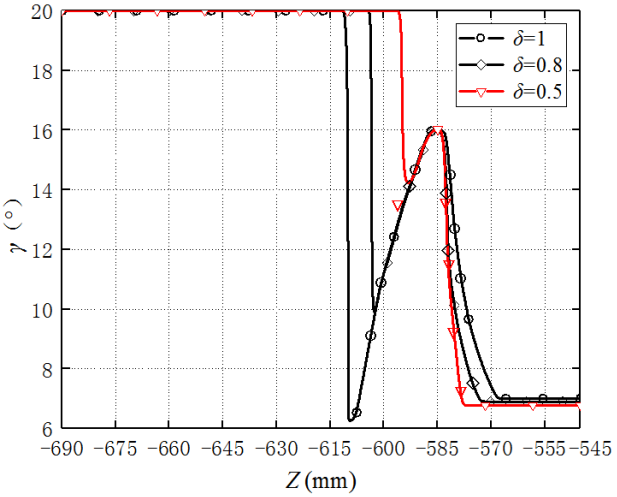

Fig.9. The variation of ladle inclination angle with different weight factors (δ=1, δ=0.8, δ=0.5)

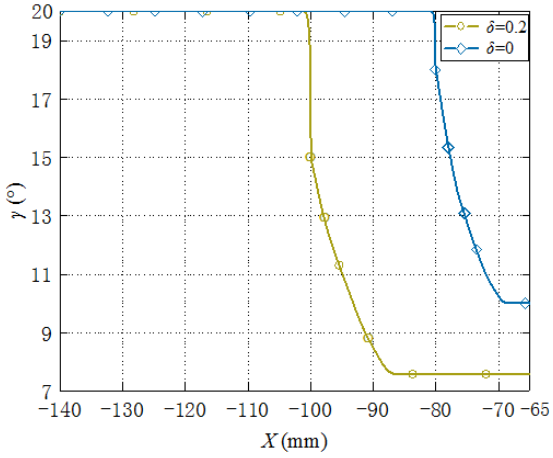

Fig.10. The variation of ladle inclination angle with different weight factors (δ=0, δ=0.2)

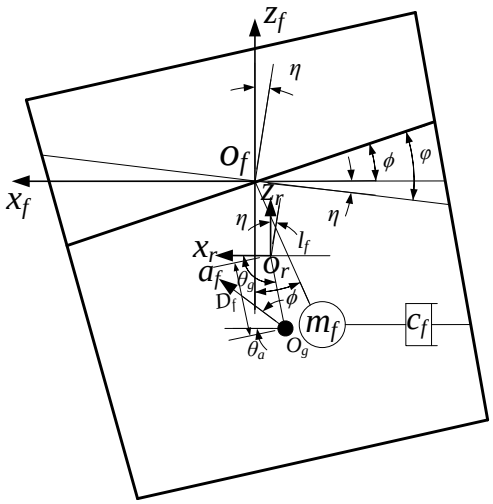

506

507 Fig.11. Pendulum sloshing model of ladle

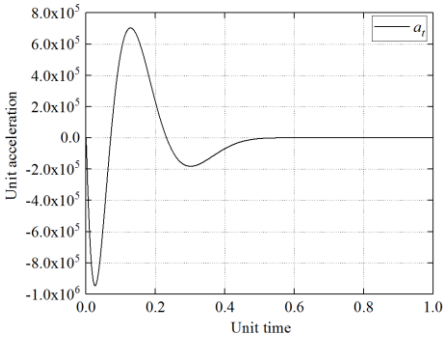

508

509 Fig.12. Unitized acceleration of global acceleration programming

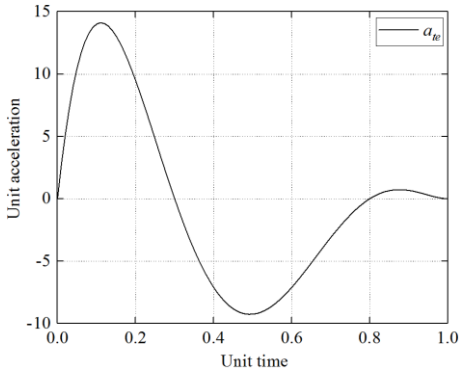

510

511 Fig.13 Unit acceleration of piecewise acceleration planning

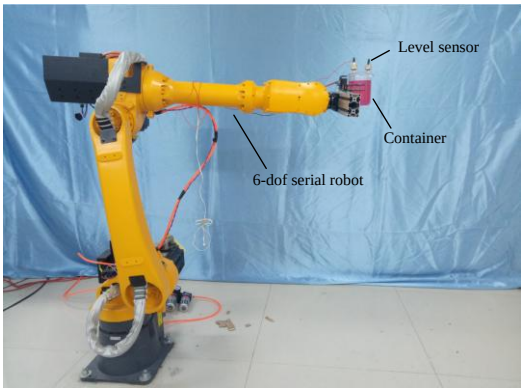

512

513 Fig.14 Experimental device for liquid sloshing

514

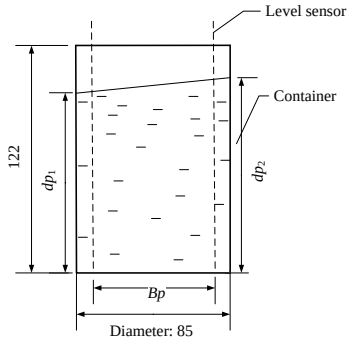

515

516 Fig.15 Schematic diagram of liquid sloshing measurement method

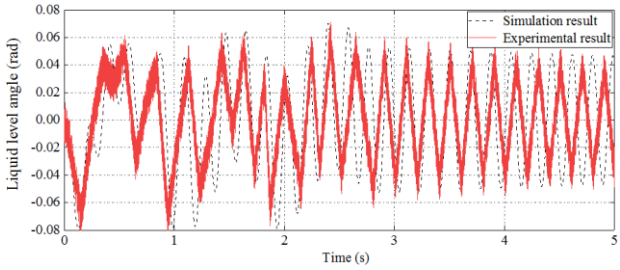

517

518 Fig.16 Simulation and experimental results of liquid sloshing at δ=0.5

519

520 0 s 1s 2s 3 s 4 s 5s

521 Fig.17 Instantaneous sloshing of liquid in experiment

522

523

524

525

526

527

528

529